

# International Conference on Space Optics—ICSO 2014

La Caleta, Tenerife, Canary Islands

7–10 October 2014

*Edited by Zoran Sodnik, Bruno Cugny, and Nikos Karafolas*



## ***Development of HgCdTe large format MBE arrays and noise-free high speed MOVPE EAPD arrays for ground based NIR astronomy***

*G. Finger*

*I. Baker*

*M. Downing*

*D. Alvarez*

*et al.*



## DEVELOPMENT OF HGCDTE LARGE FORMAT MBE ARRAYS AND NOISE-FREE HIGH SPEED MOVPE EAPD ARRAYS FOR GROUND BASED NIR ASTRONOMY

G. Finger<sup>1</sup>, I. Baker<sup>2</sup>, M. Downing<sup>1</sup>, D. Alvarez<sup>1</sup>, D. Ives<sup>1</sup>, L. Mehrgan<sup>1</sup>, M. Meyer<sup>1</sup>, J. Stegmeier<sup>1</sup>, H. J. Weller<sup>2</sup>  
<sup>1</sup>European Southern Observatory, Garching, Germany. <sup>2</sup>Selex ES Ltd, Southampton, United Kingdom.

### I. INTRODUCTION:

Large format near infrared HgCdTe 2Kx2K and 4Kx4K MBE arrays have reached a level of maturity which meets most of the specifications required for near infrared (NIR) astronomy. The only remaining problem is the persistence effect which is device specific and not yet fully under control. For ground based multi-object spectroscopy on 40 meter class telescopes larger pixels would be advantageous.

For high speed near infrared fringe tracking and wavefront sensing the only way to overcome the CMOS noise barrier is the amplification of the photoelectron signal inside the infrared pixel by means of the avalanche gain. A readout chip for a 320x256 pixel HgCdTe eAPD array will be presented which has 32 parallel video outputs being arranged in such a way that the full multiplex advantage is also available for small sub-windows. In combination with the high APD gain this allows reducing the readout noise to the subelectron level by applying nondestructive readout schemes with subpixel sampling. Arrays grown by MOVPE achieve subelectron readout noise and operate with superb cosmetic quality at high APD gain. Efforts are made to reduce the dark current of those arrays to make this technology also available for large format focal planes of NIR instruments offering noise free detectors for deep exposures. The dark current of the latest MOVPE eAPD arrays is already at a level adequate for noiseless broad and narrow band imaging in scientific instruments.

### II. LARGE FORMAT HGCDTE MBE ARRAYS:

Ground-based infrared astronomy is limited to the atmospheric windows between  $\lambda=0.8\mu\text{m}$  and  $25\mu\text{m}$ . The near infrared regime ( $\lambda=0.8\mu\text{m}$  to  $5\mu\text{m}$ ) with the Z,Y,J, H, K, L and M band windows is covered by the intrinsic InSb or HgCdTe arrays operating at temperatures between  $T=30\text{K}$  and  $80\text{K}$ . For the mid infrared in the N band ( $\lambda=8\mu\text{m}$  -  $14\mu\text{m}$ ), 1Kx1K HgCdTe arrays with a cut-off wavelength of  $\lambda_c=12\mu\text{m}$  at  $T=77\text{K}$  may present an interesting alternative to extrinsic SiAs. If the HgCdTe is cooled down from  $T=77\text{K}$  to  $T=30\text{K}$ , the cutoff wavelength shifts from  $\lambda_c=12\mu\text{m}$  to  $14\mu\text{m}$ .

As shown in Table 1, for the extremely large telescope (ELT) a large number of affordable 4Kx4K near infrared detectors are needed in the wavelength range of  $0.8\text{-}5\mu\text{m}$  [1]. This wavelength range will be covered by HgCdTe arrays with cutoff wavelengths ranging between  $\lambda_c=1.7\mu\text{m}$  to  $5.3\mu\text{m}$ . Depending on the progress of development of  $\lambda_c=1.7\mu\text{m}$  HgCdTe material which usually has poorer performance than that of material with  $\lambda_c=2.5\mu\text{m}$ , the longer cutoff  $\lambda_c=2.5\mu\text{m}$  material might also be chosen for instruments which do not include the K-band such as the ELT-PCS. Different growth processes on different substrates have been developed for large format NIR focal planes. The best performance has been achieved with MBE and LPE material grown on CdZnTe substrates which provide an ideal lattice match for  $\lambda_c=5\mu\text{m}$  HgCdTe. Diffusion limited dark currents have been demonstrated down to temperatures of  $60\text{K}$ . Excellent performance is also achieved with  $\lambda_c=2.5\mu\text{m}$  HgCdTe with dark currents of a few electrons/pixel/hour. However, the CdZnTe substrate is expensive and it is difficult to grow substrates for array formats exceeding 4Kx4K. Therefore, other substrates are in development such as silicon or GaAs which would allow a further increase of the array format. Another promising substrate for very large HgCdTe detector formats currently being developed at Raytheon is silicon.

To date the large NIR focal planes have been equipped with mosaics of 2Kx2K arrays (HAWK-I,VISTA), but the system complexity of the huge ELT focal planes demands formats of at least 4Kx4K even though larger formats would simplify system engineering aspects. The arrays are packaged on a molybdenum base to minimize the thermal mismatch, but SiC is replacing molybdenum. The progress of CMOS technology provides excellent yields for large scale multiplexers which initially was a major concern for 4Kx4K arrays. To increase the readout speed the multiplexers currently provide 64 parallel video outputs. This allows employing multiple sampling techniques to reduce the readout noise. Novel reference pixel subtraction schemes in the ROIC design facilitate the implementation of a true differential analog acquisition chain with off-chip cryogenic preamplifiers. In Fig. 1 the detector cross section of HxRG arrays is shown. The photodiodes are p-on-n double layer planar heterostructures grown by molecular beam epitaxy (MBE) on a CdZnTe substrate which is removed after bump bonding to eliminate fringing and to improve the quantum efficiency at short wavelengths. On the left side of Fig. 3 the SiC package of the 4Kx4K Hawaii-4RG array is shown. Instead of an ASIC, a symmetric

32channel cryogenic preamplifier next to the focal plane is used at ESO to port the video signal over a true differential signal chain to the ADC of the NGC controller over the and flex cables and the hermetic connector as shown on the right side of Fig. 3. Fast and slow cryogenic preamplifiers are available for the 100KHz and the 5MHz outputs of the HxRG arrays.

The selection of the technology for the large ELT focal planes will depend both on performance and cost. The performance requirements for high resolution spectroscopy and for broadband imaging may be quite different. A competitive tender may be issued to manufacture prototypes before placing the final contracts. The quantum efficiency, dark current and readout noise of near infrared arrays is almost perfect as can be seen in Fig. 2, Fig. 4 and Fig. 5. The readout noise of deep exposures with more than one hundred Fowler pairs starts to rise on infrared active pixels, but further drops on reference pixels (see solid and dash-dotted curves in Fig. 5). This demonstrates that the readout noise is not limited by the CMOS multiplexer or the rest of the acquisition chain, but by the low frequency noise of the infrared diodes.

The biggest remaining problem of large format NIR arrays are the latent images in long low flux exposures. Latent charge, or “persistence,” is the remaining signal apparent in a series of deep low flux dark exposures. It is produced in dark exposures by exposure to a bright source in previous images. Any process which, after some delay, releases charge into the conduction band can contribute to persistent images. Persistence is a function of incident flux during a previous exposure, the duration of the bright exposures, the time elapsed since the bright source was switched off, the applied reverse bias voltage and the temperature.

Decaying persistent images can also be generated in darkness without prior exposure to bright light by changing the bias voltage selectively in a subwindow of the array using the guide mode feature of the Hawaii-2RG. The change of bias voltage in the guide mode window emulates exposure to bright light which also changes the bias voltage due to photon generated discharge of the integrating capacitance. Persistent images generated by prior exposure to light or by a prior change of the bias voltage inside the guide window have the same decay time constant [3]. Therefore, persistence was attributed to traps being exposed to majority carriers in the shrinking volume of the depletion region on bright pixels. In subsequent dark exposures the populated traps release charge and generate persistent images [2]. However, this mechanism only partially explains the persistence. On some devices the effect of exposure to optical light is much stronger than the effect of changing the bias voltage in darkness.

In Fig. 6 the time decay of persistent images of 4 Hawaii-2RG arrays is compared. Black diamonds show the latent images of the first Hawaii-2RG array with the serial number #50 delivered to ESO in 2004. This array was installed in the VLT instrument SINFONI. The curves with green triangles, red asterisks and blue diamonds show the persistence of the Hawaii-2RG arrays delivered in 2010 which are installed in the KMOS instrument having serial numbers #184, #211 and #212. It is remarkable that arrays #184 and #211 from different lots exhibit similar persistence whereas array #212 has higher persistence than array #211 even though both are from the same lot. The data sheets of the KMOS arrays provided by the manufacturer show the same persistence for all three KMOS detectors and do not represent relevant data for an observational scenario at the telescope. The data of Fig. 6 represent a series of 300 second dark exposures taken with 122 nondestructive readouts for each exposure as used for deep on sky observations, whereas the manufacturer only takes a short series of 10 second exposures. In terms of persistence little progress has been made since 2004 and the problem is not yet fully under control. Global reset de-trapping is a mitigating strategy using the observing overheads to release trapped charge by keeping all reset switches closed as soon as science exposures are finished [3]. Mitigating the persistence effect will become more of an issue with the ELT, since the combination of the large telescope diameter and diffraction limited adaptive optics will increase the flux of sky lines or bright stars.

Pixels larger than  $15\mu\text{m}$  may be of interest for Multi-Object Adaptive Optics (MOAO) Integral Field spectrographs, since MOAO will not reach the diffraction limit over the large field. It will be important to get a large fraction of the energy in a single pixel. The challenge will be to increase the pixel size with a minimum increase of the capacitance of the integrating node.

Table 1 Detector requirements for the roadmap of E-ELT instruments.

Instrument	No. of Detectors	Pixel Format	Wavelength Range
MICADO	13-16	4k x 4k	0.8-2.5um
HARMONI	8	4k x 4k	0.95-2.45um
	8	4k x 4k	0.47-0.95um
METIS	1	1k x 1k	5-28um
	6	2k x 2k	3-5um
ELT-MOS	6	4k x 4k	0.6-1.7um
	6-8	4k x 4k or 6k x 6k	0.37-1.0um
ELT-HIRES	3	4k x 4k	0.8-2.45um
	5	9k x 9k	0.3-0.8um
ELT-PCS	4	4k x 4k	0.95-1.65um
	8	4k x 2k	0.6-0.9um

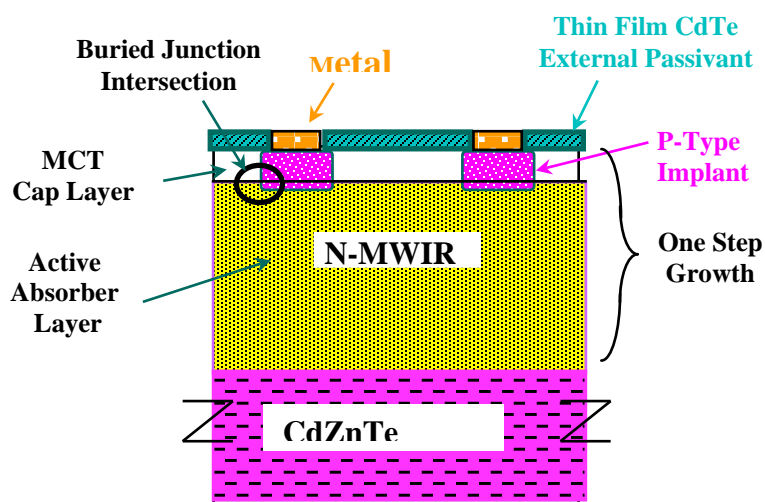


Fig. 1. Detector cross section of HxRG p-on-n Double Layer Planar Heterostructure photodiode array grown by molecular beam epitaxy (MBE)

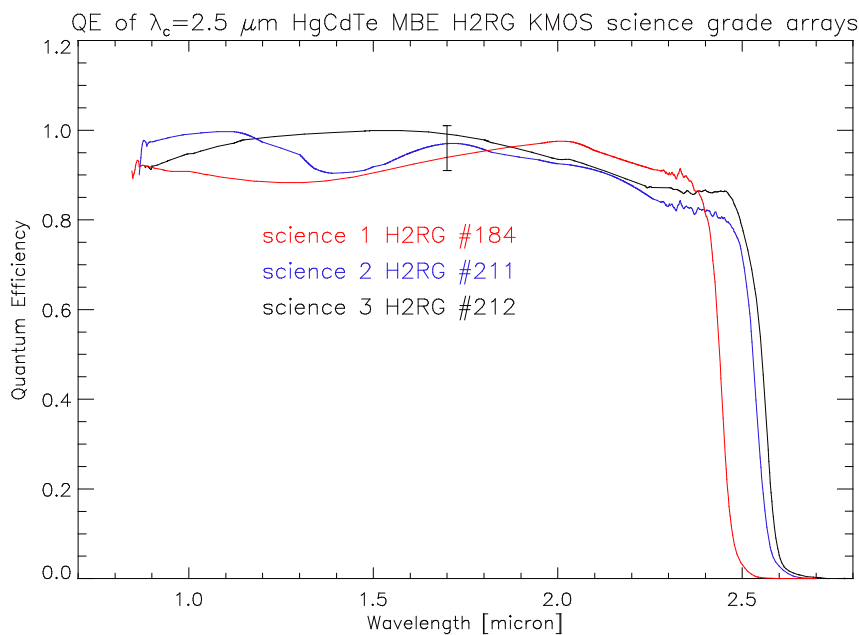
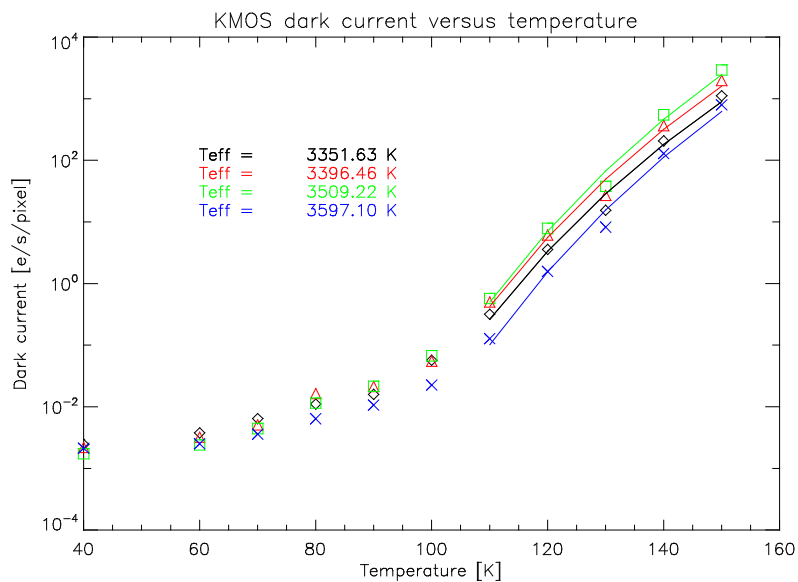


Fig. 2. Quantum efficiency versus wavelength for the three  $\lambda_c=2.5\mu\text{m}$  KMOS Hawaii-2RG arrays



**Fig. 3.** Left: SiC package of 4Kx4K Hawaii-4RG array. Right: 32-channel cryogenic preamplifier and flex cables with hermetic connector for 2Kx2K Hawaii-2RG array.



**Fig. 4.** Dark current versus temperature for the three  $\lambda_c=2.5\mu\text{m}$  KMOS Hawaii-2RG arrays. Generation-recombination limited operation is obtained at  $T>100\text{K}$ .

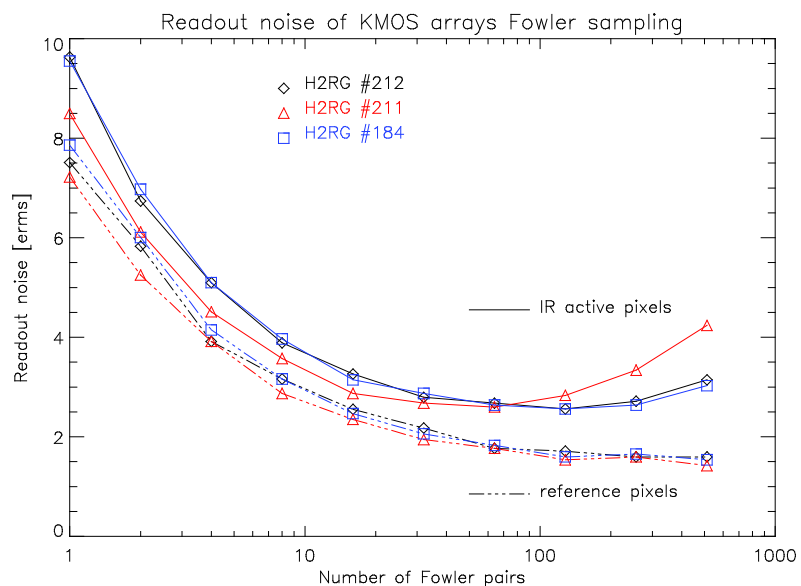


**Fig. 5.** Readout noise versus number of Fowler pairs for the three  $\lambda_c=2.5\mu\text{m}$  KMOS Hawaii-2RG arrays. Solid line: infrared pixels. Dash-dotted line: reference pixels.

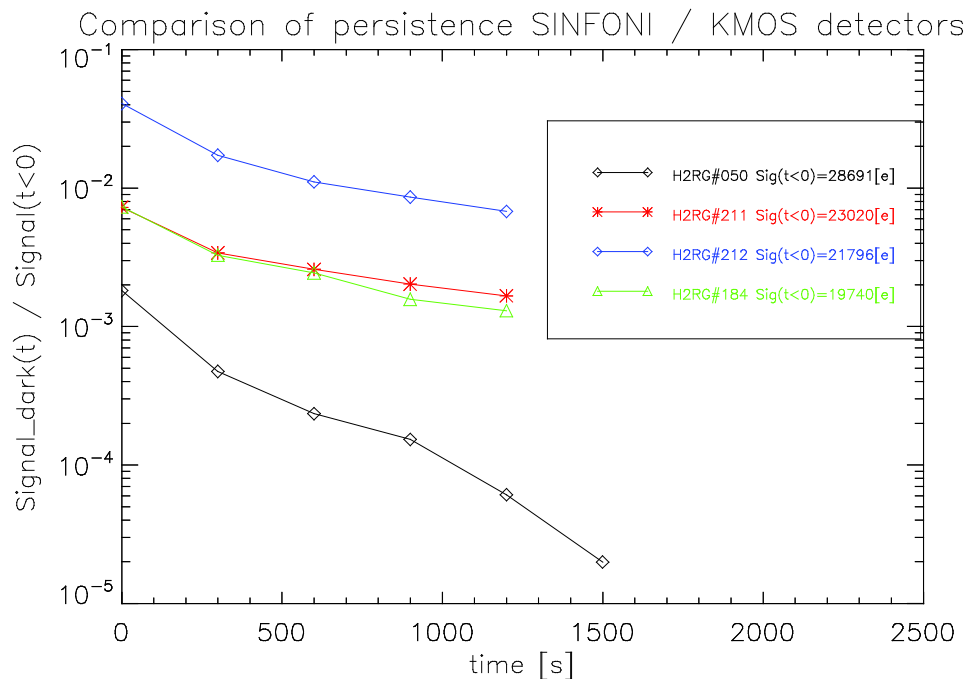


**Fig. 6.** Comparison of the persistence of 4 Hawaii-2RG arrays. Black diamonds: First Hawaii-2RG array #50 delivered in 2004 and installed in SINFONI. Green triangles, red asterisks and blue diamonds: Hawaii-2RG arrays delivered in 2010 and installed in KMOS. Remark: arrays #184 and #211 from different lots have similar persistence whereas array #212 has higher persistence than array #211 even though they are from the same lot.

### III. HIGH SPEED NOISE FREE MOVPE EAPD ARRAYS:

For NIR wavefront sensors in adaptive optics (AO) systems and fringe trackers in interferometers high frame rates of > 1KHz are needed to compensate atmospheric effects efficiently. Due to high read noise (70 erms) at fast frame rates with more than 1 Mpix/s/output, the use of conventional IR detectors for AO applications has been mainly restricted to low order Tip Tilt and “Truth” sensors which require small format size and modest read out speeds of 100 fps. These arrays use a source follower in the unit cell. In the past decade improvements in CMOS technology have only marginally reduced the readout noise at high speed even if capacitive transimpedance amplifiers (CTIA) have been used to amplify the signal in the unit cell. This impasse can be broken if the signal is amplified before it is integrated onto the silicon readout. CTIA amplifiers in the unit cell of the readout multiplexer are not practical in small pixel sizes so attention has turned to electron multiplication by an impact ionisation effect – the so-called avalanche photodiode array (APD). The APD gain process in HgCdTe is almost noiseless because HgCdTe, contrary to silicon, is a direct semiconductor. Phonons are not needed to generate an electron-hole pair. Furthermore, in HgCdTe the mass of the electron is much smaller than the mass of the holes and the gain process is then mainly due to pure electron multiplication resulting in a noiseless, deterministic avalanche gain process. The excess noise factor measured with an array from SELEX is 1.23 up to an APD gain of 79.

Developments over the past 5 years at Leti LIR and SELEX have now made these devices available to the astronomy community [4][5]. ESO has funded the APD development at SELEX which is discussed in this paper. The need for low breakdown currents at high voltages requires a mature device technology which is best achieved with Metal Organic Vapour Phase Epitaxy (MOVPE). MOVPE alternates the growth of CdTe and HgCd and the bandgap of Hg<sub>(1-x)</sub>Cd<sub>x</sub>Te after interdiffusion is determined by the ratio x. In this way MOVPE allows the band structure and doping to be controlled on a 0.1µm scale and provides more flexibility for the design of diode structures. Low cost GaAs substrates provide a wafer-scale process suitable for large area arrays. Dopants are introduced on the CdTe cycle so the doping levels are independent of the bandgap. Iodine is used as a donor and arsenic as an acceptor. The resulting design of the diode structure and the band diagram is shown in Fig. 7 and Fig. 8. The GaAs substrate is removed after hybridization to the multiplexer. The top layer diode structure is CdTe. The next layer is a wide bandgap HgCdTe buffer layer followed by the p-type absorber layer. The wide bandgap buffer layer limits the spectral response at the short wavelength side to λ > 1.3 µm. The

absorber layer has a cutoff wavelength of  $\lambda_c=2.6 \mu\text{m}$ . Each pixel is electrically isolated by a mesa slot that extends through the absorber to eliminate lateral collection. The widening of the bandgap around the edges of the absorber effectively separates carriers from surface states and minimizes junction currents where the junction intercepts the sidewall. The absorber and the gain region are decoupled so each can be optimized separately. The n-type gain region is made narrow bandgap to give high gain per volt. The gain region is electrically connected at the bottom to the unit cell of the silicon Readout Integrated Circuit (ROIC) by standard indium bump technology.

The special requirements of adaptive optics and interferometry with multiple windows and low readout noise at high frame rates could only be met by developing the new SAPHIRA ROIC, which is described in more detail in a previous paper [4]. The SAPHIRA ROIC has a format of 320x256 pixels, a pixel pitch of 24  $\mu\text{m}$  and 32 parallel video outputs operating at 5 MHz. The 32 outputs are organized in such a way that they simultaneously read out 32 adjacent pixels in a row. The readout time of a full frame is 500 $\mu\text{s}$ , allowing frame rates of 1 kHz for double correlated sampling. With this readout topology, windowed readout schemes benefit from the multiplex advantage of 32 parallel channels. This is one of the key features of the SAPHIRA ROIC which helps to achieve the lowest readout noise. Depending on the size of the window many frames can be read out nondestructively with typical integration times of 1 ms, to reduce the readout noise even further with Fowler sampling. A 10 MHz 32-channel ADC board in the NGC detector front end electronics allows real-time digital filtering and Fowler preprocessing in the FPGA of the ADC board to limit the required bandwidth of the fiber link to the real time computer.

The development work at SELEX resulted in several wafers of MOVPE material hybridized on the SAPHIRA ROIC and the best science-grade arrays were delivered to ESO and the NRC Herzberg Institute (HI) of Canada for further evaluation. The test setup used at ESO to evaluate the eAPD arrays was also described in an earlier SPIE paper [6]. A test camera housing a cryogenically cooled f/11 Offner relay with two cold filter wheels images a warm test pattern such as a grid of holes illuminated by an extended blackbody onto the detector. The test pattern shown in Fig. 9 was taken with the test pattern in front of an extended blackbody at a temperature of 70°C observing with the H band filter. The flux in the holes of the test pattern is 1.12 photons/ms per pixel. The integration time is 1.17ms. The left image of Fig. 9 shows a single double correlated sampling (DCS) exposure, and the right image is the average of 12 chop cycles at a chopping frequency of 10 Hz. The left image clearly demonstrates that the sensitivity of the detector is sufficient to detect single photons in a single frame at the maximum APD gain of 79 using simple DCS.

The main advantage of the SAPHIRA readout topology only becomes apparent when reading out small subwindows, as are often needed for low order AO systems and fringe trackers. For example, the GRAVITY wavefront sensor has 9x9 sub-apertures with 8x8 pixels per sub-aperture [8]. Therefore, a window of only 96x72 pixels needs to be read out. Because of the ROIC topology, the number of pixels in the fast readout direction has to be a multiple of 32. In Fig. 10 the readout noise is plotted versus the number of nondestructive samples for different APD gains ranging from 25 to 79. The integration time for the data points of Fig. 10 having less than 8 nondestructive readouts (4 Fowler pairs) is fixed to 500 $\mu\text{s}$ , to limit the number of interrupts for the host computer. For 16 (Fowler-8) and more nondestructive readouts the integration time increases with the number of nondestructive readouts. The integration time is 1.17 ms for 32 readouts (16 Fowler pairs) and 37.5 ms for 1024 readouts. For integration times longer than 19 ms or more than 256 Fowler pairs the readout noise becomes independent of the APD gain and is dominated by the instrumental photon background in our camera. The noise data were taken at a detector temperature of 85 K. With Fowler-16, an APD gain of 79 and an integration time of 1.17 ms, the readout noise is 0.2 electrons rms. With this performance the read noise of the SAPHIRA array in the GRAVITY wavefront sensor is negligible and single photons can safely be detected.

The quantum efficiency (QE) of the SAPHIRA array is temperature dependent. The QE in K-band rises from 0.65 to 0.72 when the temperature is increased from T=85 to 100K. The dark current at a temperature of T=85K and an APD gain of 40 is 0.04 electrons/ms which is negligible for wavefront sensors with integration times in the range of milliseconds. But also for ground based narrow and broad band imaging in H and K band with sky flux levels generating photocurrents of hundred to a few thousand electrons per second this performance already sufficient sufficient to generate noise free photon shot noise limited images. Only for high resolution spectroscopy the dark current of eAPD detectors has to be further reduced by more than two orders of magnitude to make them competitive with conventional large format NIR arrays.

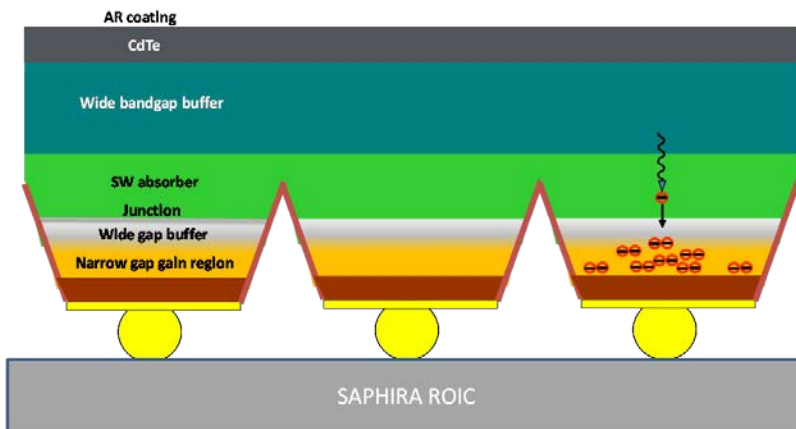


Fig. 7. Diode structure of metal organic vapour phase epitaxy (MOVPE)

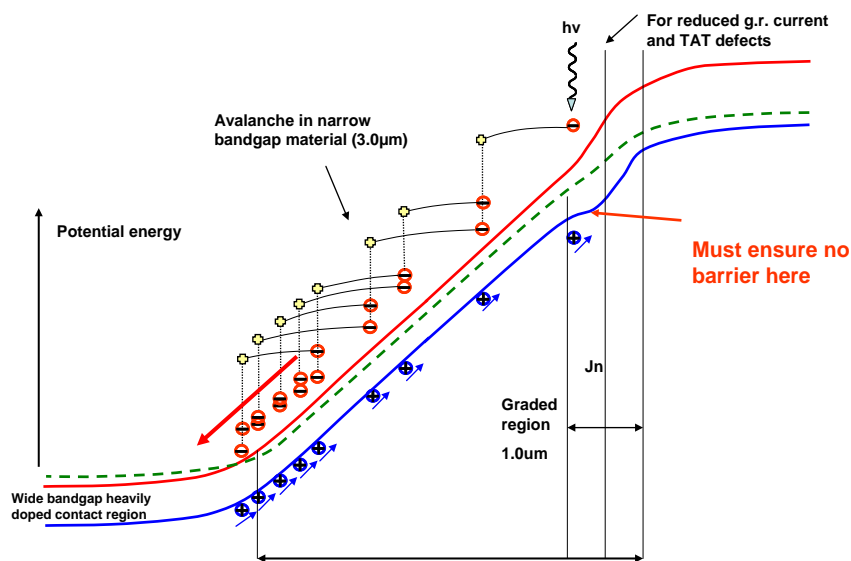


Fig. 8.: Band diagram of MOVPE heterostructure eAPD array. Wide bandgap in absorber region and the junction on the right side. Narrow bandgap in gain region for maximum APD gain at small bias voltages.

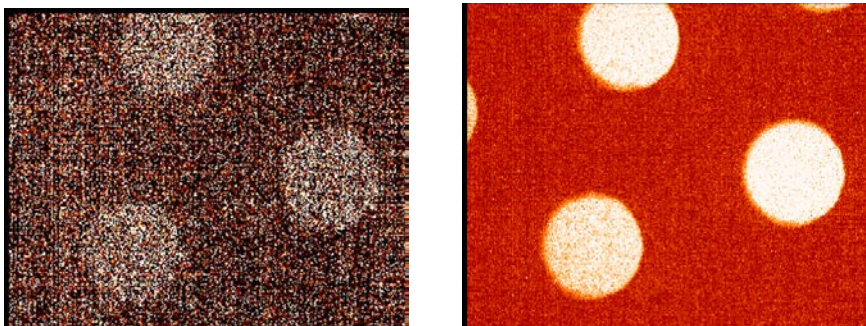
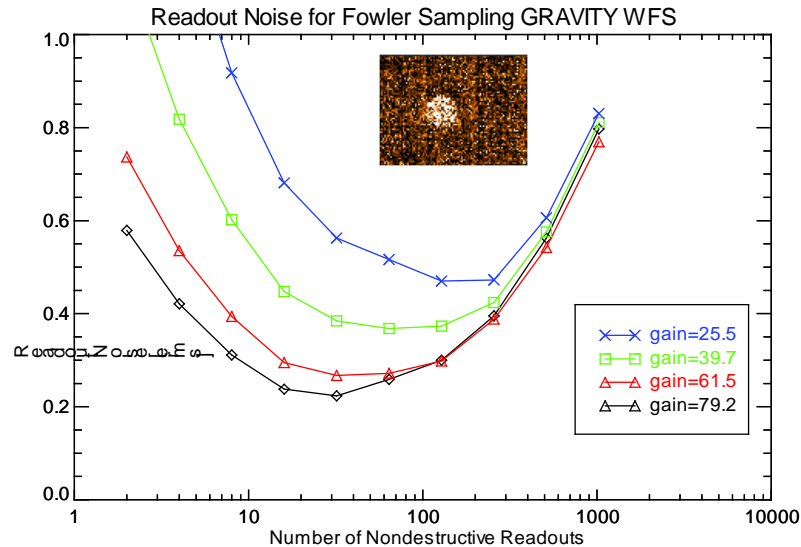


Fig. 9. H-band test pattern with signal difference of 1.3 photons or 0.59 electrons in integration time of 1.17ms. Left: Single exposure. Right: Mean of chopped image.



**Fig. 10.** Readout noise of the 96x72 pixel sub-window of the GRAVITY wavefront sensor with Fowler sampling as a function of the number of nondestructive readouts at different APD gains. Integration time increases with the number of nondestructive readouts. The inserted image in the top right corner shows a single 1ms exposure imaging a circular test pattern having a signal of 1 electron/ms/pixel.

#### IV. CONCLUSIONS:

Large format 4Kx4K MBE arrays fulfill most of the requirements of 8 meter class and future extremely large telescopes. However, the persistence of these arrays is still an unsolved problem which will be aggravated by the high flux due to the large collecting area of the ELT and due to diffraction limited performance of its adaptive optics.

In the near infrared electron avalanche photodiodes grown by MOVPE have already reached a performance level adequate to deploy noise free high speed detectors in wavefront sensors and fringe trackers. They can already be used for noise free high time resolution imaging in H and K band and have already been used for NIR lucky imaging [7]. Further development is needed to provide APD devices with panchromatic response and dark current levels compliant with flux levels of  $\sim 10^{-2}$  photons/s/pixel, as encountered in high resolution spectrographs.

#### REFERENCES

- [1] M. Downing, G. Finger, D. Ives, O. Iwert, J. Kolb and S. Ramsay, "Detector developments at ESO to prepare for the E-ELT era", *Proc SPIE*, vol 9154, Montreal, in press, 2014.
- [2] R. Smith, M. Zavodny, G. Rahmer and M. Bonati, "A theory for image persistence in HgCdTe photodiodes", *Proc. SPIE vol 7021*, High Energy, Optical, and Infrared Detectors for Astronomy III, 2008.
- [3] G. Finger, R. Dorn, S. Eschbaumer, D. Ives, L. Mehrgan, M. Meyer and J. Stegmeier, "Recent Performance Improvements, Calibration Techniques and Mitigation Strategies for Large-format HgCdTe Arrays", [http://www.eso.org/sci/meetings/2009/dfa2009/Presentations/Finger\\_Wednesday\\_09\\_20.ppt](http://www.eso.org/sci/meetings/2009/dfa2009/Presentations/Finger_Wednesday_09_20.ppt), Detectors for Astronomy, Garching, 2009.
- [4] G. Finger, I. Baker, D. Alvarez, D. Ives, L. Mehrgan, M. Meyer, J. Stegmeier and H. Weller, "SAPHIRA detector for infrared wavefront sensing", *Proc SPIE*, vol 9148, Montreal, in press, 2014.
- [5] P. Feautrier, P. et al., "Revolutionary visible and infrared sensor detectors for the most advanced astronomical AO systems", *Proc SPIE*, vol 9148, Montreal, in press, 2014.
- [6] G. Finger, I. Baker, R. Dorn, S. Eschbaumer, D. Ives, L. Mehrgan, M. Meyer, J. Stegmeier, "Development of high-speed, low-noise NIR HgCdTe avalanche photodiode arrays for adaptive optics and interferometry", *Proc. SPIE vol 7742*, pp. 7742, 2010.
- [7] D. Atkinson D. and D. Hall, "Characterization and applications of SAPHIRA HgCdTe APDs at the University of Hawai'i", *Proc SPIE*, vol 9146, Montreal, in press, (2014).
- [8] F. Eisenhauer F. et al., "GRAVITY: Observing the Universe in Motion", *The Messenger*, vol. 143, p. 16-24, (2011).